

## Electronic Supporting Information (ESI)

### Position- and region-isomerized derivatives of a V-shaped fluorophore: the unique solution-state dual emission and the unusual force-induced solid-state turn-on emission

Hong-Yu Fu, Xiao-Jing Liu, Hao Zha, Xiao-Xue Li, Yi Xu, Fan Yang and Min Xia\*

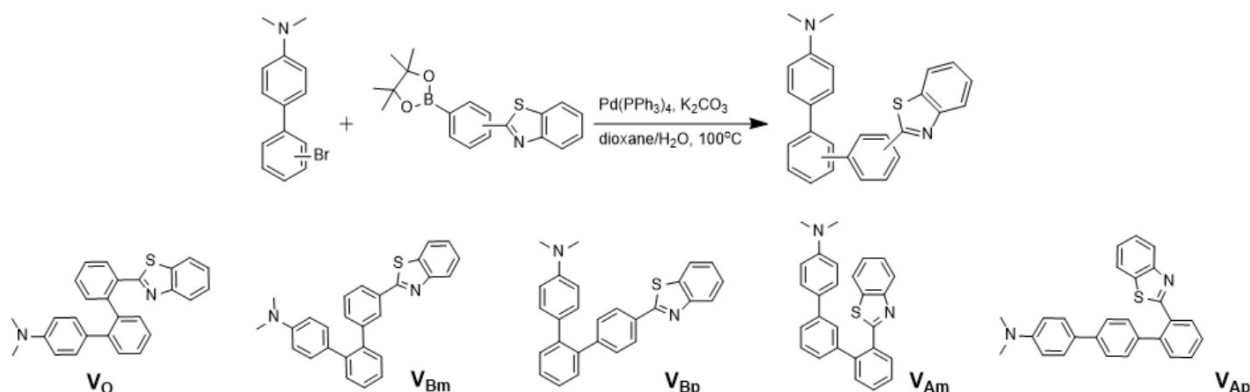
Department of Chemistry, Zhejiang Sci-Tech University, Hangzhou, 310018

E-mail: [xiamin@zstu.edu.cn](mailto:xiamin@zstu.edu.cn)

#### Materials and instruments

All the reagents were analytically pure and some chemicals were further purified by recrystallization or distillation. Melting points were determined by an OptiMelt automated melting point system. The  $^1\text{H}$  NMR (400 MHz) and  $^{13}\text{C}$  NMR (100 MHz) spectra were obtained on a Bruker Avance II DMX 400 spectrometer with  $\text{CDCl}_3$  as the solvent. The absorption spectra were measured on a Shimadzu UV 2501(PC)S UV-Vis spectrometer, and the fluorescence spectra were acquired on a Perkin-Elmer LS55 spectrophotometer. The quantum yields were measured with quinine sulfate in 0.1 M sulfuric acid solution ( $\Phi_f=0.55$ ) as the reference and the solid-state quantum yields were gained by an integral sphere. The mass spectrum was recorded on a HP 1110 mass spectrometer. The crystallographic data were determined on a Bruker Gemini Ultra diffractometer with a CCD counter. The powder X-ray diffraction patterns were recorded on DX2700 with  $\text{Cu-K}\alpha$  radiation operating at 40 kV and 40 mA by a  $0.3^\circ/\text{min}$  scanning rate. The preparation of compound **V** was referred to our previous report (*RSC Adv.*, **2017**, 7, 50720–50728).

#### Synthetic procedures



At room temperature and N<sub>2</sub> flux, the solution of 2'- or 3'- or 4'-bromo-N,N-dimethyl-[1,1'-biphenyl]-4-amine (12 mmol, 3.3 g) in dioxane / H<sub>2</sub>O (4:1, v/v, 10 mL) was injected into the mixture of 2-[2- or 3- or 4-(4,4,5,5-tetramethyl-1,3,2-dioxaborolan-2-yl)phenyl]benzo[d]thiazole (10 mmol, 3.37 g), Pd(PPh<sub>3</sub>)<sub>4</sub> (0.5 mmol, 0.577 g) and K<sub>2</sub>CO<sub>3</sub> (15 mmol, 2.07g) in dioxane/H<sub>2</sub>O (4:1, v/v, 20 mL). The resulted mixture was heated at 100°C for 24 h and then cooled to room temperature. After filtration, the filtrate was diluted with water and extracted by CH<sub>2</sub>Cl<sub>2</sub> (3×15 mL). The combined organic layers were dried over anhydrous Na<sub>2</sub>SO<sub>4</sub>. After the removal of solvent, the residue was purified on a silica gel column chromatography to offer the corresponding product.

2''-(benzo[d]thiazol-2-yl)-N, N-dimethyl-[1,1': 2',1''-terphenyl]-4-amine (**V<sub>O</sub>**): 67% yield, white powder; m.p. 150.9-152.3 °C; <sup>1</sup>H NMR (400MHz, CDCl<sub>3</sub>) δ 2.90(s, 6H), 6.44(d, *J*=8.4 Hz, 2H), 6.80(d, *J*=8.8 Hz, 2H), 7.30-7.36(m, 2H), 7.38-7.51(m, 7H), 7.74(d, *J*=8.0 Hz, 1H), 8.79(d, *J*=8.0 Hz, 1H), 8.11-8.13(m, 1H); <sup>13</sup>C NMR (100MHz, CDCl<sub>3</sub>) δ 40.43, 111.89, 121.21, 123.05, 124.62, 125.68, 126.60, 127.32, 128.58, 129.78, 129.83, 130.02, 130.20, 131.70, 131.92, 133.07, 136.55, 138.16, 141.60, 142.01, 149.02, 152.64, 167.25; EI-MS(70 eV) *m/z* (%) 406(M<sup>+</sup>, 100), 392(48), 376(12), 362(10), 286(25), 271(15), 254(5), 228(7), 202(8).

3''-(benzo[d]thiazol-2-yl)-N, N-dimethyl-[1,1': 2',1''-terphenyl]-4-amine (**V<sub>Bm</sub>**): 74% yield, white powder; m.p. 160.4-161.7°C; <sup>1</sup>H NMR (400MHz, CDCl<sub>3</sub>) δ 3.02(s, 6H), 6.79(d, *J*=8.0 Hz, 2H), 7.24(d, *J*=7.6 Hz, 1H), 7.35(t, *J*=8.0 Hz, 1H), 7.40(t, *J*=8.0 Hz, 1H), 7.47(m, 3H), 7.51-7.62(m, 5H), 7.74(d, *J*=8.0 Hz, 1H), 8.11(d, *J*=8.4 Hz, 1H), 8.18(dd, *J*<sub>1</sub>= 7.6 Hz, *J*<sub>2</sub>=2 Hz, 1H); <sup>13</sup>C NMR (100MHz, CDCl<sub>3</sub>) δ 40.64, 112.82, 121.38, 123.20, 124.87, 125.65, 125.87, 127.68, 127.73, 127.87, 128.69, 130.03, 130.35, 130.89, 132.75, 136.76, 140.53, 141.10, 141.97, 149.94, 152.78, 167.84; EI-MS(70 eV) *m/z* (%) 406(M<sup>+</sup>, 100), 391(45), 376(10), 362(15), 273(17), 254(7), 227(15), 202(5).

4''-(benzo[d]thiazol-2-yl)-N,N-dimethyl-[1,1':2',1''-terphenyl]-4-amine (**V<sub>Bp</sub>**): 81% yield, pale yellow powder; m.p. 183.4-185.2°C; <sup>1</sup>H NMR (400MHz, CDCl<sub>3</sub>) δ 3.06(s, 6H), 6.86(d, *J*=8.4 Hz, 2H), 7.33-7.40(m, 3H), 7.48(dd, *J*<sub>1</sub>=1.2 Hz, *J*<sub>2</sub>=8.0 Hz, 1H), 7.53(dt, *J*<sub>1</sub>=2 Hz, *J*<sub>2</sub>=8.0 Hz, 2H), 7.56(t, *J*=2Hz, 1H), 7.58-7.62(m, 4H), 7.76(d, *J*=8.0 Hz, 1H), 8.11(d, *J*=8.0 Hz, 1H), 8.13(dd, *J*<sub>1</sub>=2Hz, *J*<sub>2</sub>=8.0 Hz, 1H); <sup>13</sup>C NMR (100MHz, CDCl<sub>3</sub>) δ 40.64, 112.87, 121.41, 123.23, 124.86, 125.85, 125.96, 127.59, 127.62, 130.07, 130.35, 130.50, 130.93, 132.73, 136.78, 137.78, 140.41, 141.67, 150.08, 152.86, 168.01; EI-MS(70 eV) *m/z* (%) 406 (M<sup>+</sup>, 100), 391(52), 376(13), 362(17), 253(8), 203(5).

2''-(benzo[d]thiazol-2-yl)-N,N-dimethyl-[1,1':3',1''-terphenyl]-4-amine (**V<sub>Am</sub>**): 61% yield, white powder; m.p. 127.6-129.2°C; <sup>1</sup>H NMR (400MHz, CDCl<sub>3</sub>) δ 2.95(s, 6H), 6.66(dd, *J*<sub>1</sub>=1.2 Hz, *J*<sub>2</sub>=7.2 Hz, 2H), 7.13(dd, *J*<sub>1</sub>=2Hz, *J*<sub>2</sub>=7.2 Hz, 2H), 7.28-7.31(m, 1H), 7.37(m, 1H), 7.41-7.57(m, 6H), 7.93(dd, *J*<sub>1</sub>=1.2 Hz, *J*<sub>2</sub>=8.0 Hz, 1H), 8.02-8.06(m, 2H), 8.12(dd, *J*<sub>1</sub>=1.2 Hz, *J*<sub>2</sub>=8.0 Hz, 1H); <sup>13</sup>C NMR (100MHz, CDCl<sub>3</sub>) δ 40.53, 112.23, 121.60, 123.22, 125.12, 125.39, 126.27, 126.79, 127.95, 128.51, 129.06, 130.59, 130.69, 132.77, 133.42, 135.15, 139.25, 140.81, 143.07, 149.32, 154.18, 168.33; EI-MS(70 eV) *m/z* (%) 406 (M<sup>+</sup>, 100), 389(35), 262(10), 254(7), 202(17).

2''-(benzo[d]thiazol-2-yl)-N,N-dimethyl-[1,1':4',1''-terphenyl]-4-amine (**V<sub>Ap</sub>**): 78% yield, yellowish green powder; m.p. 183.1-184.6°C; <sup>1</sup>H NMR (400MHz, CDCl<sub>3</sub>) δ 2.91(s, 6H), 6.59(d, *J*=7.6 Hz, 2H), 7.03(d, *J*=8.4 Hz, 2H), 7.31(d, *J*=8.0 Hz, 2H), 7.35-7.49(m, 6H), 7.88(d, *J*=8.0 Hz, 1H), 7.96(d, *J*=8.0 Hz, 2H), 8.04(d, *J*=8.4 Hz, 1H); <sup>13</sup>C NMR (100MHz, CDCl<sub>3</sub>) δ 40.38, 112.04, 121.61, 123.10, 125.09, 126.30,

126.74, 127.18, 128.00, 130.46, 130.52, 130.62, 130.67, 131.45, 135.03, 139.22, 140.77, 145.18, 149.22, 154.18, 168.12; EI-MS(70 eV)  $m/z$  (%) 406( $M^+$ , 100), 389(33), 316(7), 286(8), 254(5), 202(13).

### X-ray structure analysis

Single crystals of the title compounds grown in MeCN/EtOH were selected for the X-ray analysis. The diffraction data were collected on a Bruker CCD area-detector diffractometer equipped with a graphite-monochromated Mo- $K_\alpha$  radiation ( $\lambda=0.71073$  Å). The unit cell parameters were determined from a least-squares refinement of the setting angles. The structure was solved by direct methods and refined on  $F^2$  by the full-matrix least-squares methods with SHELXS-97. The refinement was carried out by full-matrix least squares method on the positional and anisotropic temperature parameters of the non-hydrogen atoms using SHELXL-97. All H atoms were placed in the idealized positions and constrained to ride on their parent atoms. Crystallographic data for compound **V** (CCDC 1551667), **V<sub>O</sub>** (CCDC 1834425), **V<sub>Bm</sub>** (CCDC 1834423), **V<sub>Bp</sub>** (CCDC 1834424) and **V<sub>Am</sub>** (CCDC 1844322) were deposited at CCDC center and can be obtained free of charge from The Cambridge Crystallographic Data Centre via [www.ccdc.cam.ac.uk/data\\_request/cif](http://www.ccdc.cam.ac.uk/data_request/cif).

**Table S1** Crystallographic data for **V<sub>O</sub>** and **V**

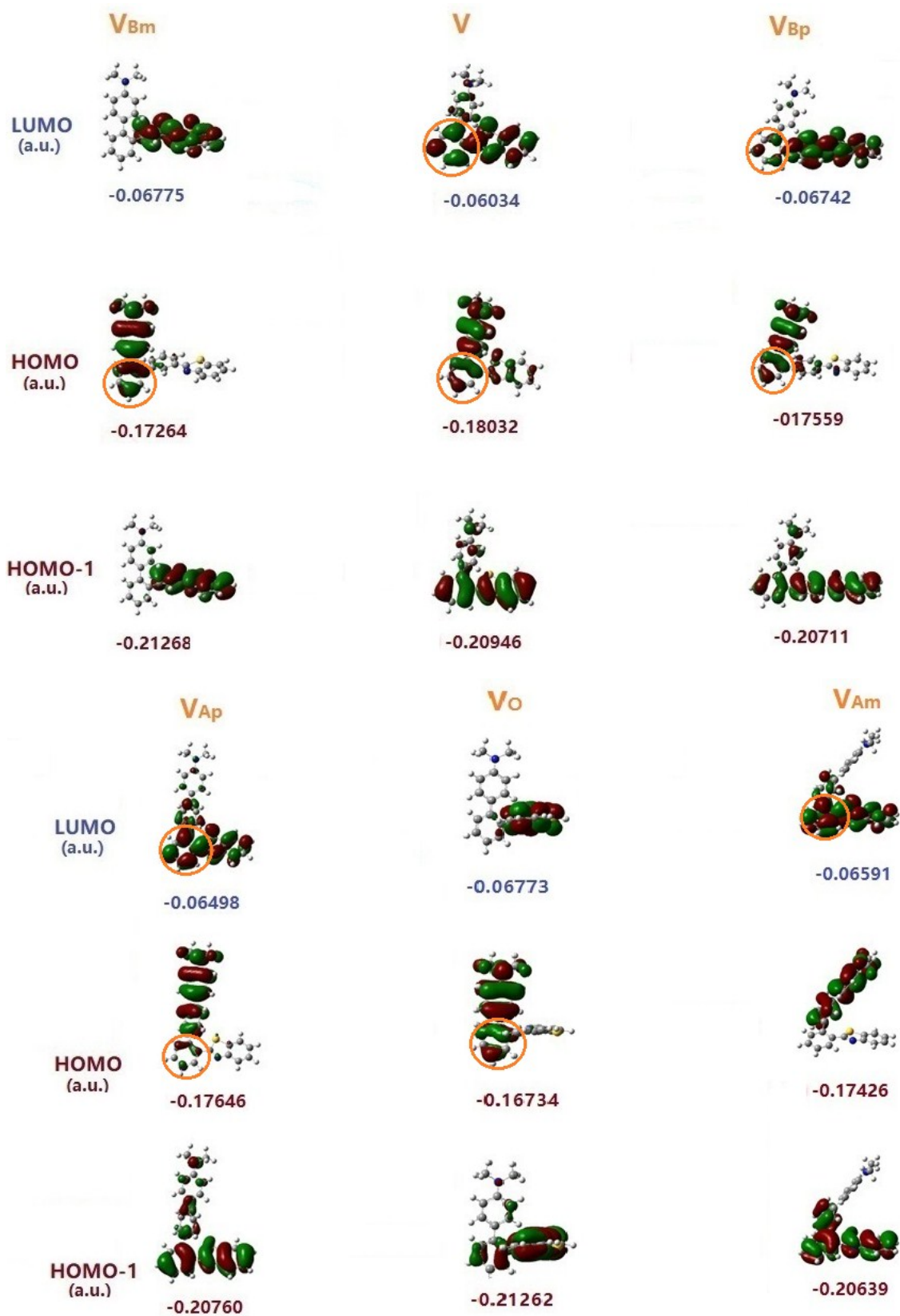
<b>V<sub>O</sub></b>		<b>V</b>
$a = 7.398(1)$ Å		$a = 6.1982(5)$ Å
$b = 14.3691(15)$ Å		$b = 24.956(2)$ Å
$c = 20.4895(16)$ Å		$c = 10.8550(9)$ Å
$\alpha = 90^\circ$	$\beta = 91.329(8)^\circ$	$\alpha = 90^\circ$
	$\gamma = 90^\circ$	$\beta = 97.234(8)^\circ$
		$\gamma = 90^\circ$
Temperature	293 K	170 K
Volume	2177.5(4)	1665.7(2)
Space group	P 2 <sub>1</sub> /n	P 2 <sub>1</sub> /c
Hall group	- P 2 <sub>yn</sub>	-P 2 <sub>ybc</sub>
Density	1.240 g/cm <sup>3</sup>	1.318 g/cm <sup>3</sup>
Z	4	4
$M_u$	0.164 / nm	0.198 / nm
$F_{000}$	856.0	696.0
$h, k, l$ (max)	8, 17, 24	7, 30, 13
$N_{ref}$	3970	3045
$T_{min}, T_{max}$	0.641, 1.000	0.766, 1.000
$R_{reflections}$	0.0641 (2040)	0.0592 (2445)
$wR^2_{reflections}$	0.1843 (3970)	0.1526(3045)
S	1.005	1.079
$N_{par}$	273	219

**Table S2** Crystallographic data for **V<sub>Bm</sub>** and **V<sub>Bp</sub>**

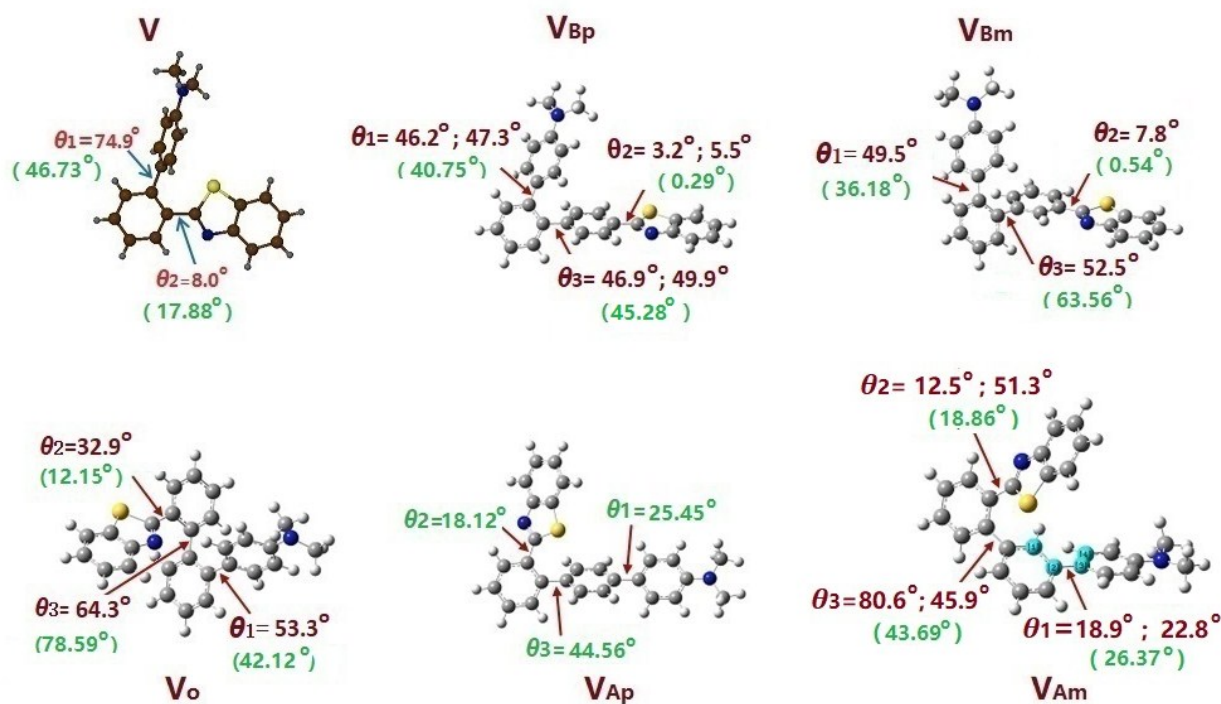
<b>V<sub>Bm</sub></b>		<b>V<sub>Bp</sub></b>	
<i>a</i> = 10.7946(7) Å		<i>a</i> = 12.2955(11) Å	
<i>b</i> = 7.7940(6) Å		<i>b</i> = 13.9512(11) Å	
<i>c</i> = 25.0193(18) Å		<i>c</i> = 12.4705(14) Å	
$\alpha = 90^\circ$	$\beta = 96.088(6)^\circ$	$\alpha = 90^\circ$	$\beta = 102.145(9)^\circ$
$\gamma = 90^\circ$		$\gamma = 90^\circ$	
Temperature	180 K	180 K	
Volume	2093.1(3)	2091.3 (3)	
Space group	P 2 <sub>1</sub> /c	P 2 <sub>1</sub>	
Hall group	- P 2 <sub>ybc</sub>	-P 2 <sub>yb</sub>	
Density	1.290 g/cm <sup>3</sup>	1.291 g/cm <sup>3</sup>	
<i>Z</i>	4	4	
<i>Mu</i>	0.171 / nm	0.171 / nm	
<i>F</i> <sub>000</sub>	856.0	856.0	
<i>h, k, l</i> (max)	13, 9, 30	14, 16, 15	
<i>N</i> <sub>ref</sub>	3809	5954	
<i>T</i> <sub>min</sub> , <i>T</i> <sub>max</sub>	0.936, 1.000	0.878, 1.000	
<i>R</i> <sub>reflections</sub>	0.0425 (2919)	0.0555 (4526)	
<i>wR</i> <sup>2</sup> <sub>reflections</sub>	0.1056 (3809)	0.1520 (5954)	
<i>S</i>	1.016	1.045	
<i>N</i> <sub>par</sub>	273	558	

**Table S3** Crystallographic data for  $V_{Am}$ 

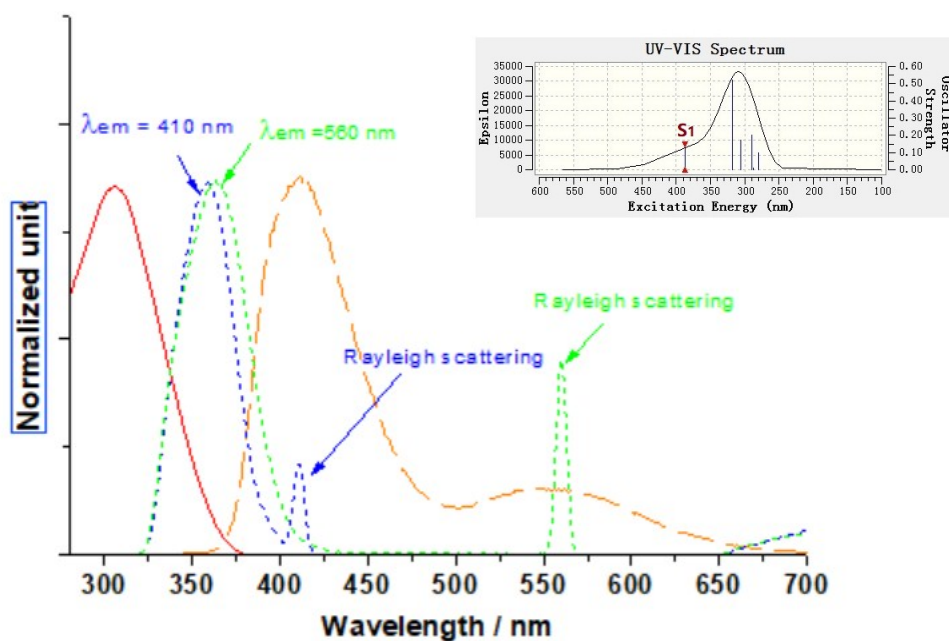
$V_{Am}$	
$a = 41.697(4) \text{ \AA}$	
$b = 11.1157(11) \text{ \AA}$	
$c = 9.2068(8) \text{ \AA}$	
$\alpha = 90^\circ$ $\beta = 93.753(6)^\circ$ $\gamma = 90^\circ$	
Temperature	293 K
Volume	4258.1(7)
Space group	P 2 <sub>1</sub> /c
Hall group	- P 2 <sub>ybc</sub>
Density	1.268 g/cm <sup>3</sup>
Z	8
$Mu$	0.168 / nm
$F_{000}$	1712.0
$h, k, l$ (max)	50, 13, 11
$N_{ref}$	7791
$T_{min}, T_{max}$	0.939, 0.978
$R_{reflections}$	0.0649 (4103)
$wR^2_{reflections}$	0.1622 (7765)
S	1.020
$N_{par}$	545



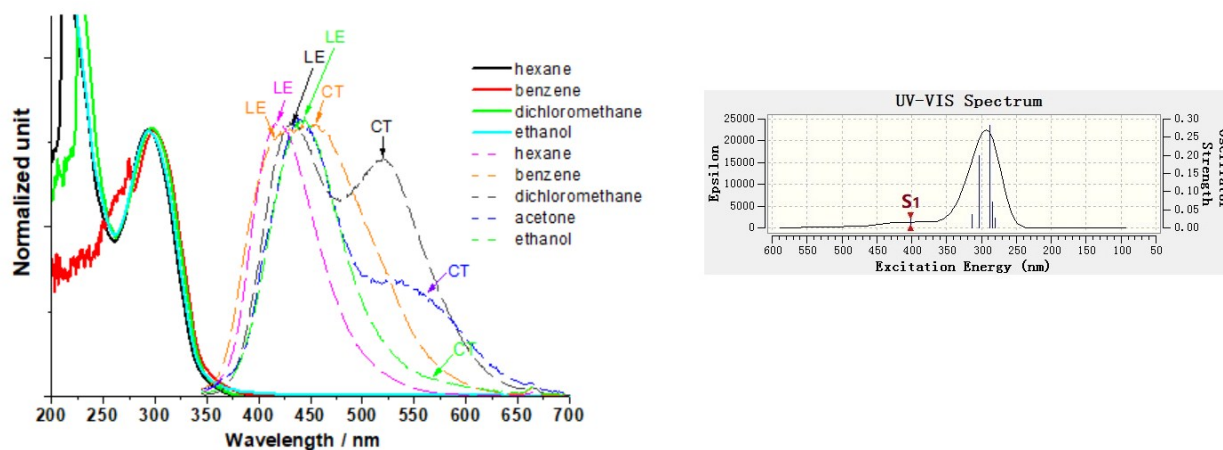
**Fig. S1** Electronic distributions on frontier molecular orbitals calculated by TD-DFT at B3LYP/6-31G (d, p) level (solid-line cycles: delocalization with electrons)



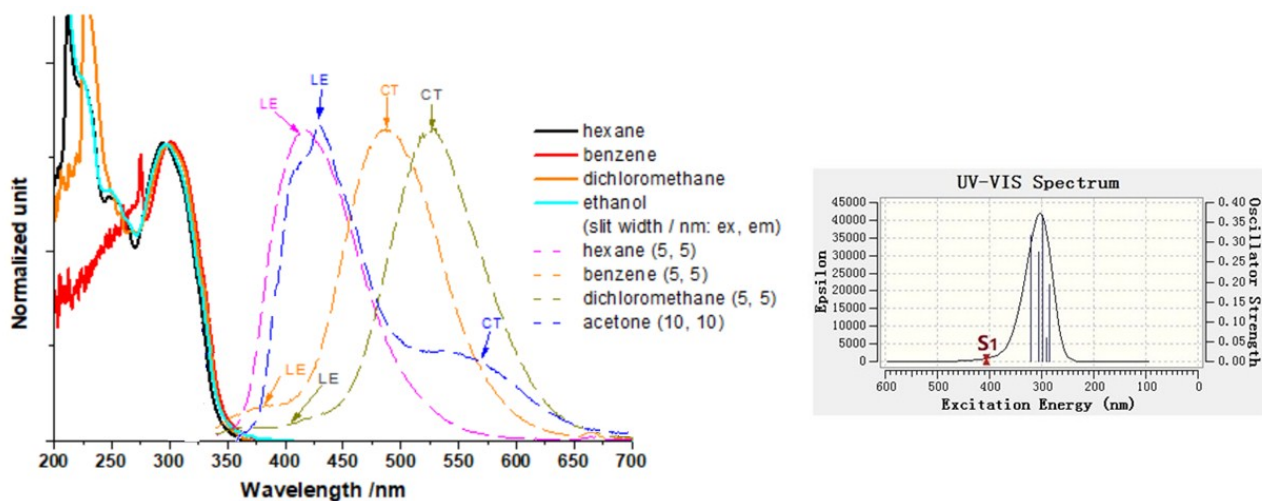
**Fig. S2** Excited-state geometries of V-shaped fluorophores in crystalline phase (red) and in gas phase (green) calculated by TD-DFT at B3LYP/6-31G (d, p) level



**Fig. S3** Absorption (solid line), excitation (dot lines) and emission (dash line,  $\lambda_{\text{ex}}=330$  nm) spectra of  $V_{\text{Ap}}$  in acetone (50  $\mu\text{M}$ ) [ *inserted*: TD-DFT calculated UV-Vis spectrum at B3LYP/6-31G(d, p) level in gas phase ]

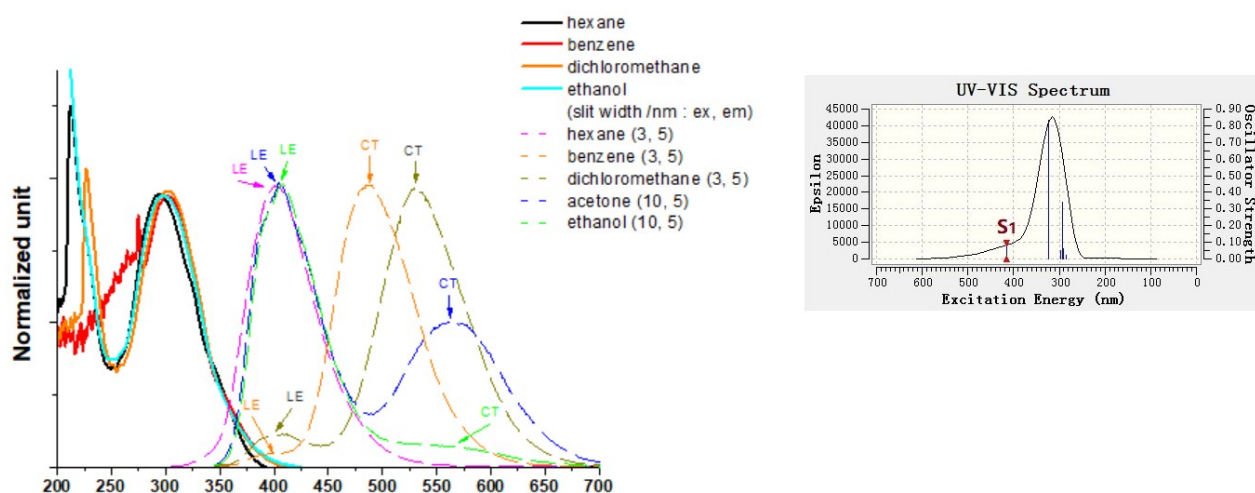


**Fig. S4** Absorption (solid lines) and emission spectra (dash lines,  $\lambda_{\text{ex}}=330$  nm, slit width / nm : ex 5; em 5) of compound **V<sub>O</sub>** (500  $\mu\text{M}$ ) in different solvents [ *inserted*: TD-DFT calculated UV-Vis spectrum at B3LYP/6-31G(d, p) level in gas phase ]

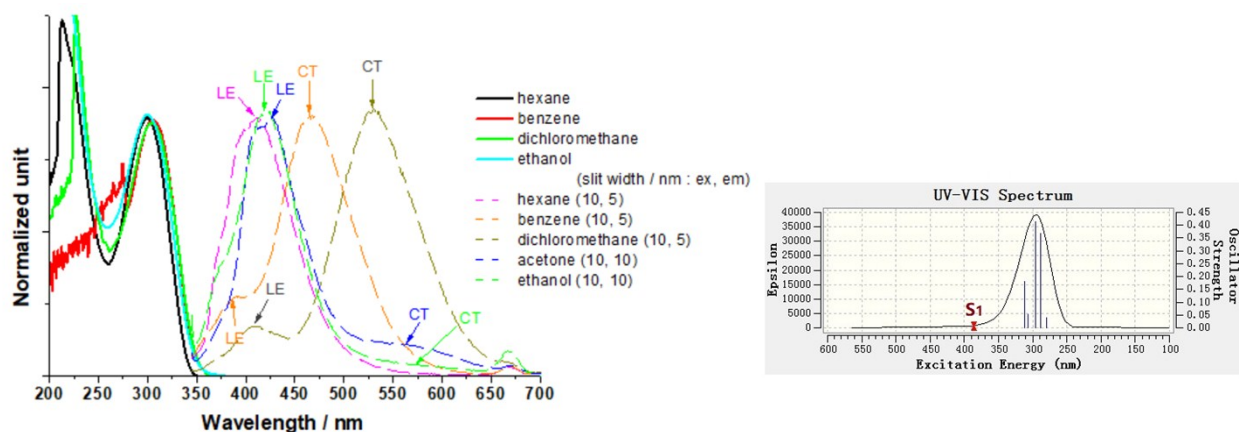


**Fig. S5** Absorption (solid lines) and emission spectra (dash lines,  $\lambda_{\text{ex}}=330$  nm) of compound **V<sub>Bm</sub>** (500  $\mu\text{M}$ ) in different solvents [ *inserted*: TD-DFT calculated UV-Vis spectrum at B3LYP/6-31G(d, p) level in gas phase ]

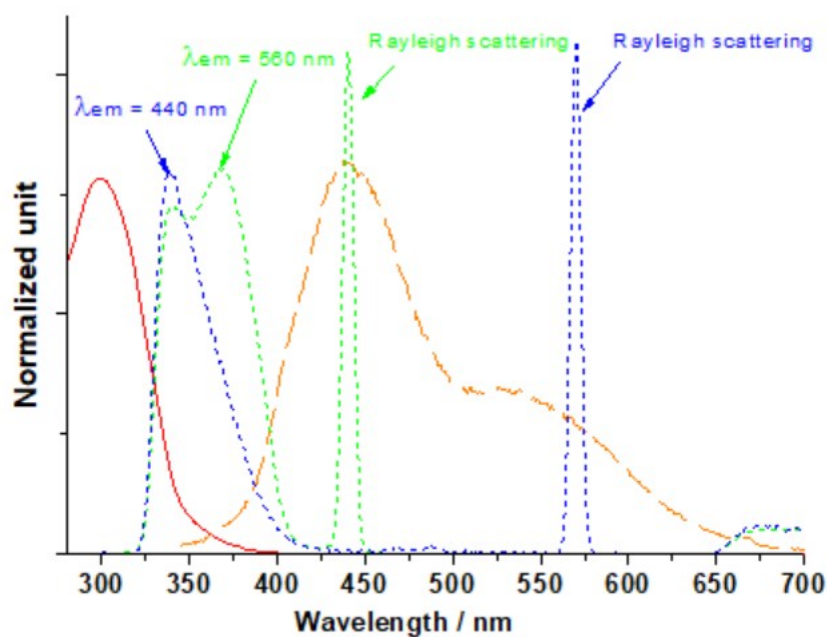




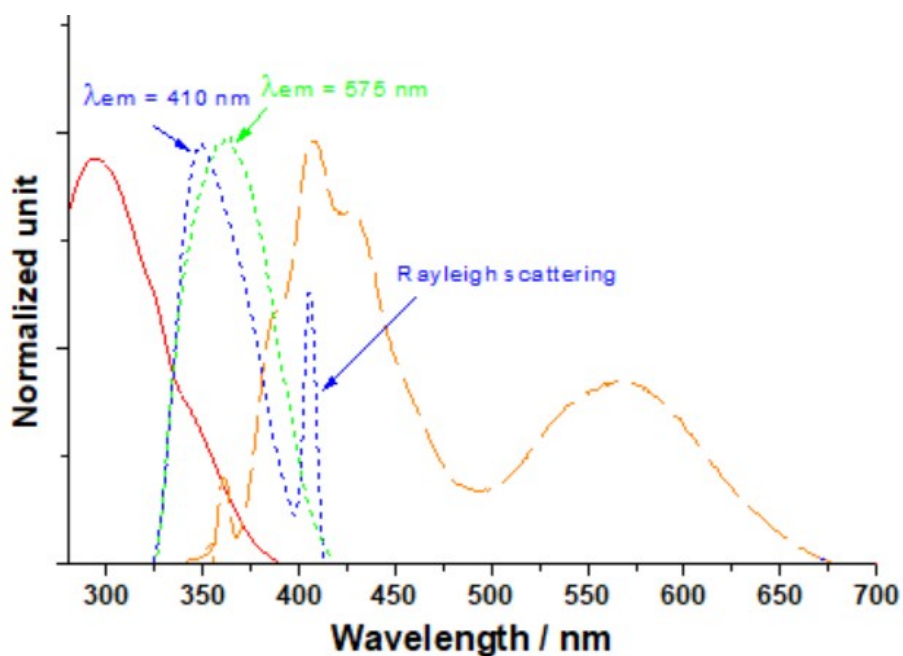
**Fig. S6** Absorption (solid lines) and emission spectra (dash lines,  $\lambda_{\text{ex}}=330$  nm) of compound **V<sub>Bp</sub>** (50  $\mu\text{M}$ ) in different solvents [ *inserted*: TD-DFT calculated UV-Vis spectrum at B3LYP/6-31G(d, p) level in gas phase ]



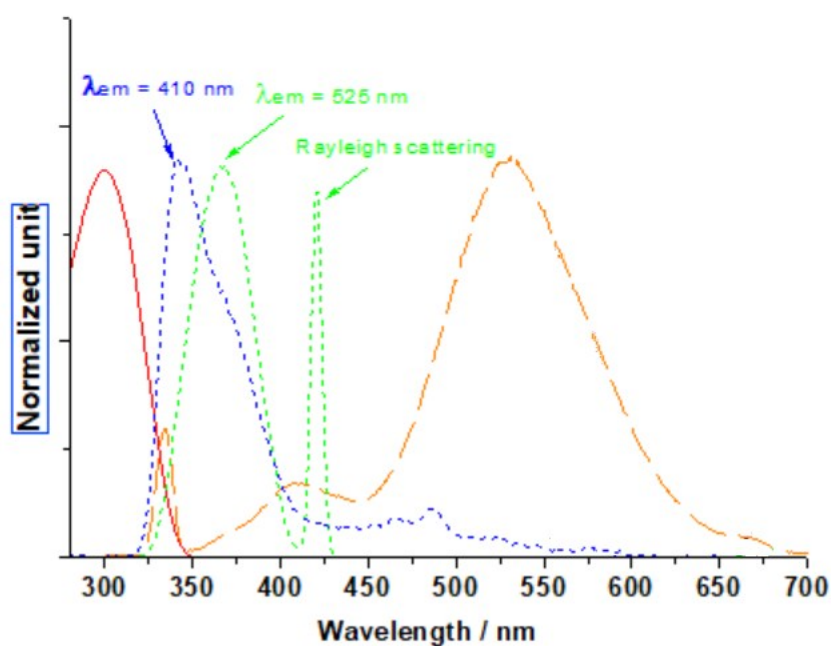
**Fig. S7** Absorption (solid lines) and emission spectra (dash lines,  $\lambda_{\text{ex}}=330$  nm) of compound **V<sub>Am</sub>** (500  $\mu\text{M}$ ) in different solvents [ *inserted*: TD-DFT calculated UV-Vis spectrum at B3LYP/6-31G(d, p) level in gas phase ]



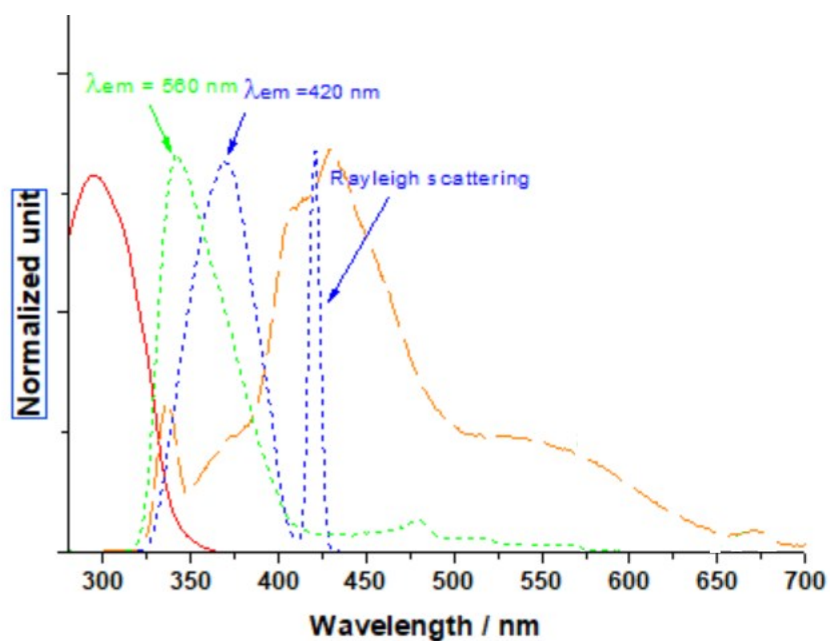
**Fig. S8** Absorption (solid line), excitation (dot lines) and emission (dash line,  $\lambda_{\text{ex}}=330$  nm) spectra of  $V_O$  in acetone (500  $\mu\text{M}$ )



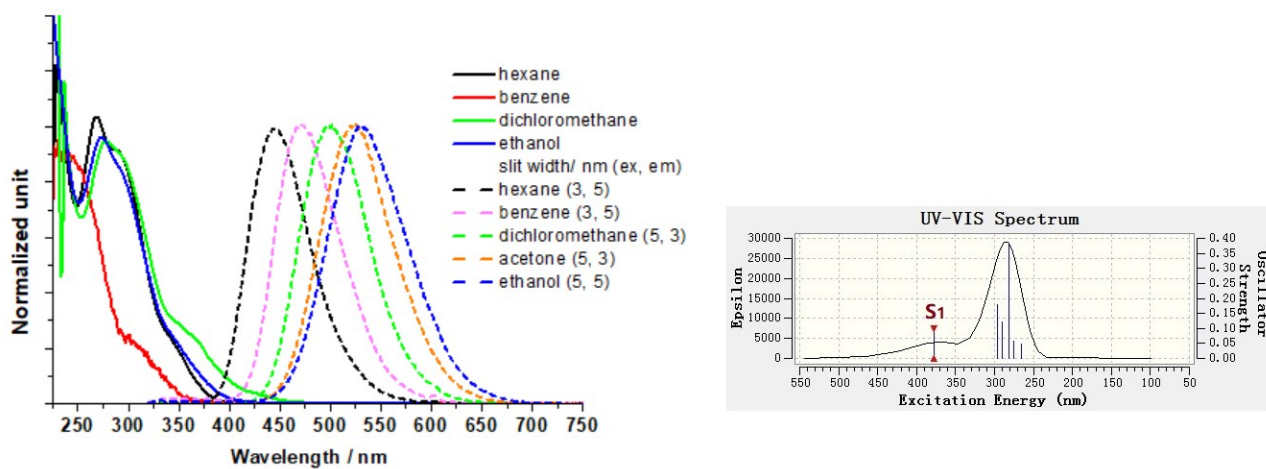
**Fig. S9** Absorption (solid line), excitation (dot lines) and emission (dash line,  $\lambda_{\text{ex}}=330$  nm) spectra of  $V_{Bp}$  in acetone (50  $\mu\text{M}$ )



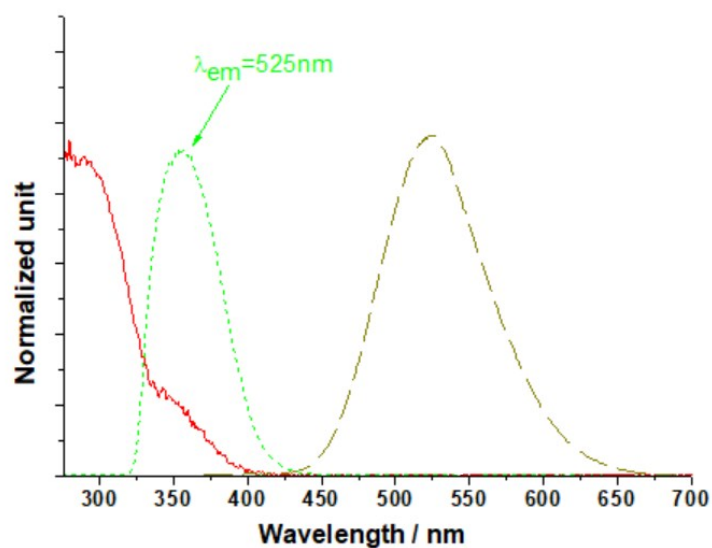
**Fig. S10** Absorption (solid line), excitation (dot lines) and emission (dash line,  $\lambda_{ex}=330$  nm) spectra of  $V_{Am}$  in acetone (500  $\mu M$ )



**Fig. S11** Absorption (solid line), excitation (dot lines) and emission (dash line,  $\lambda_{ex}=330$  nm) spectra of  $V_{Bm}$  in acetone (500  $\mu M$ )



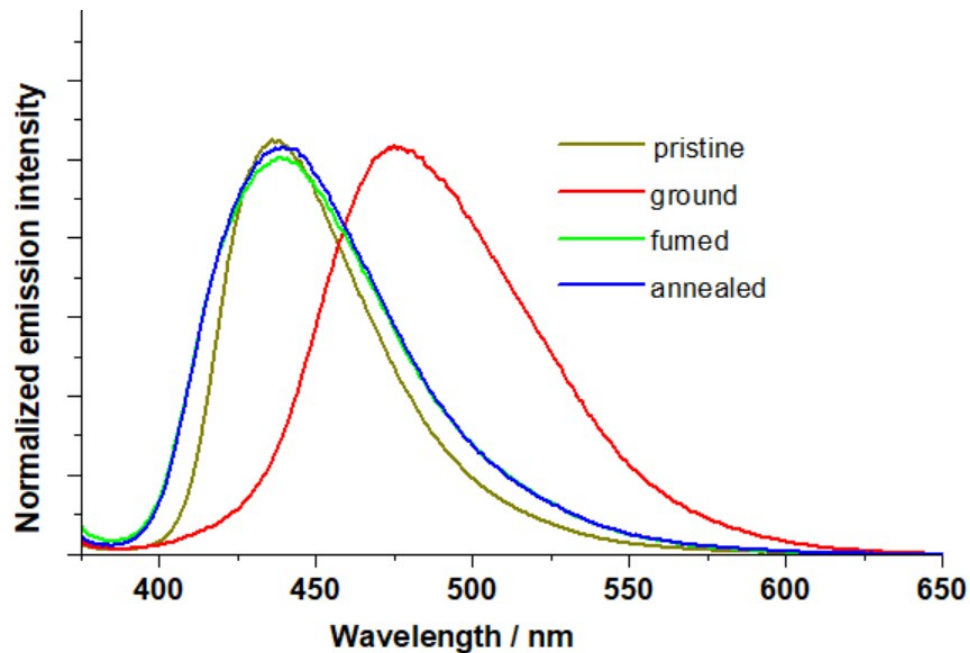
**Fig. S12** Absorption (solid lines) and emission spectra (dash lines,  $\lambda_{\text{ex}}=350$  nm) of compound **V** (50  $\mu\text{M}$ ) in different solvents [ *inserted*: TD-DFT calculated UV-Vis spectrum at B3LYP/6-31G(d, p) level in gas phase]



**Fig. S13** Absorption (solid line), excitation (dot lines) and emission (dash line,  $\lambda_{\text{ex}}=350$  nm) spectra of **V** (50  $\mu\text{M}$ ) in acetone

**Table S1** Emission wavelengths of compounds in different solvents <sup>a</sup>

Compd.	<i>n</i> -hexane		benzene		dichloromethan		acetone		ethanol	
	e									
<b>V</b>	---- <sup>b</sup>	<i>445</i>	---- <sup>b</sup>	<i>471</i>	---- <sup>b</sup>	<i>498</i>	---- <sup>b</sup>	<i>522</i>	---- <sup>b</sup>	<i>531</i>
<b>V<sub>O</sub></b>	<u>409</u>	---- <sup>c</sup>	<u>410</u>	<i>447</i>	<u>426</u>	<i>520</i>	<u>430</u>	<i>538</i>	<u>430</u>	---- <sup>c</sup>
<b>V<sub>Am</sub></b>	<u>406</u>	---- <sup>c</sup>	<u>392</u>	<i>467</i>	<u>406</u>	<i>530</i>	<u>414</u>	<i>560</i>	<u>416</u>	---- <sup>c</sup>
<b>V<sub>Ap</sub></b>	<u>412</u>	---- <sup>c</sup>	<u>395</u>	<i>487</i>	<u>406</u>	<i>526</i>	<u>410</u>	<i>558</i>	<u>410</u>	---- <sup>c</sup>
<b>V<sub>Bm</sub></b>	<u>410</u>	---- <sup>c</sup>	<u>392</u>	<i>453</i>	<u>413</u>	<i>528</i>	<u>424</u>	<i>556</i>		
<b>V<sub>Bp</sub></b>	<u>402</u>	---- <sup>c</sup>	<u>393</u>	<i>489</i>	<u>400</u>	<i>532</i>	<u>403</u>	<i>565</i>	<u>403</u>	<i>575</i>

<sup>a</sup> underlined: LE emission; italic: TICT emission.<sup>b</sup> not existent<sup>c</sup> cannot be observable**Fig. 14** Emission spectra ( $\lambda_{\text{ex}}=365$  nm) of compound **V** under different solid-state conditions

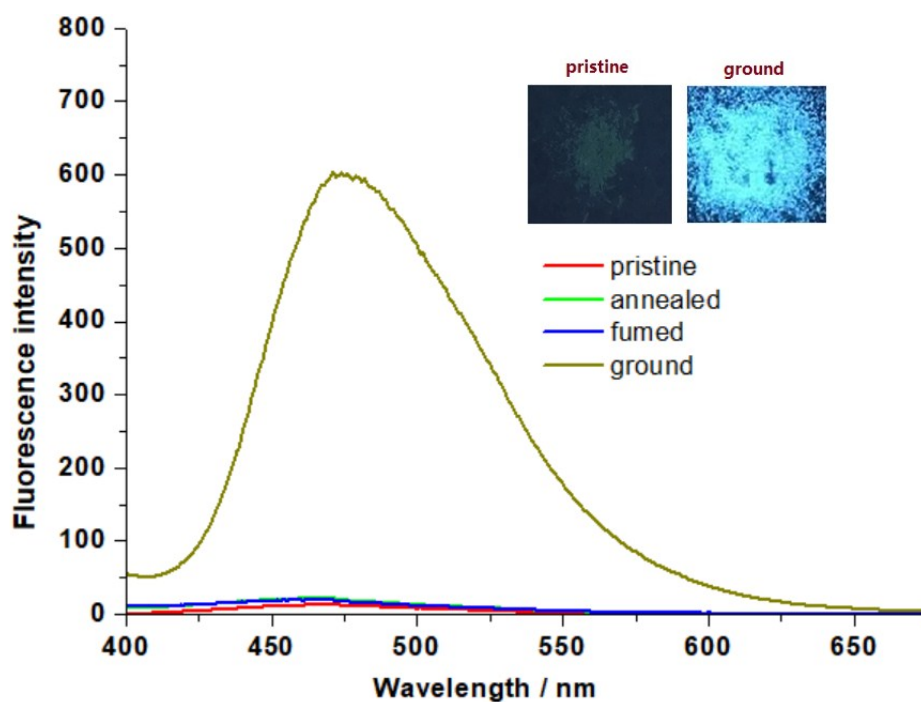


**Fig. 15** Emission spectra ( $\lambda_{\text{ex}} = 365$  nm) and photos of compound  $\mathbf{V}_O$  under different solid-state conditions (photos were taken under 365 nm UV light)

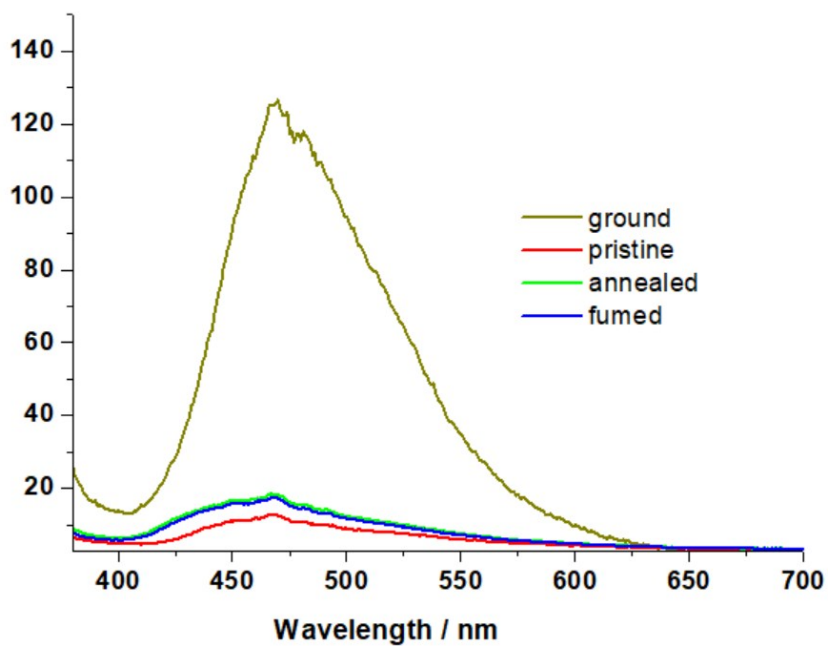


**Fig. 16** Emission spectra ( $\lambda_{\text{ex}} = 365$  nm) of compound  $\mathbf{V}_{Am}$  under different solid-state conditions



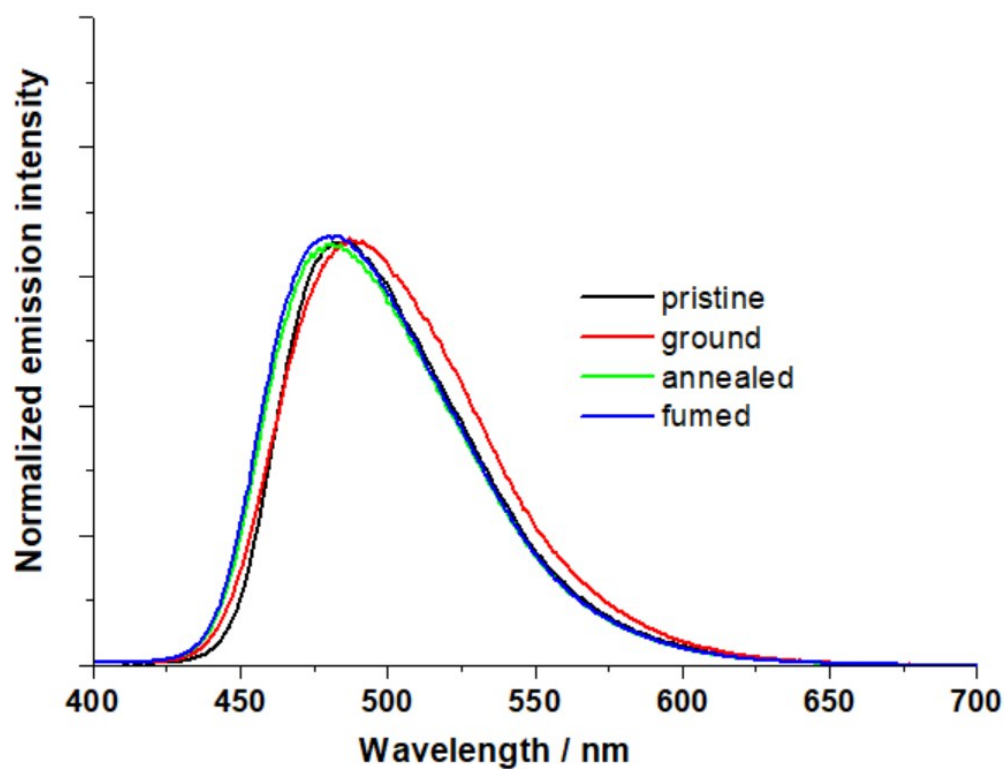


Fig. 17 Emission spectra ( $\lambda_{\text{ex}} = 365$  nm) of compound  $\text{V}_{\text{Bp}}$  under different solid-state conditions

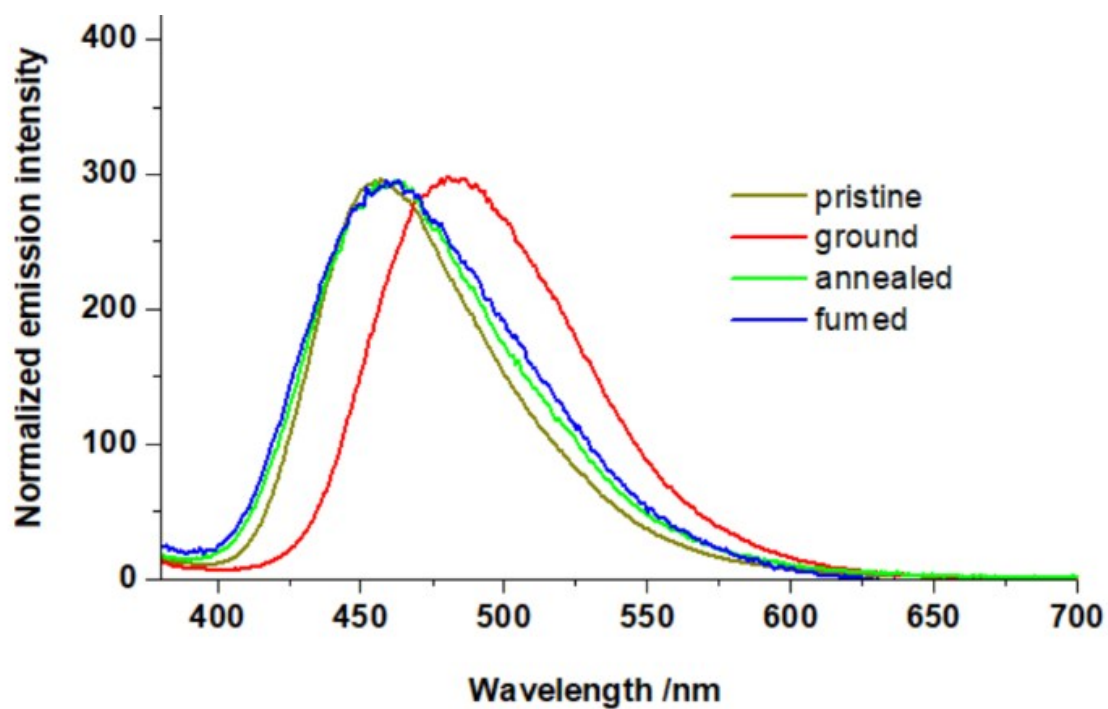
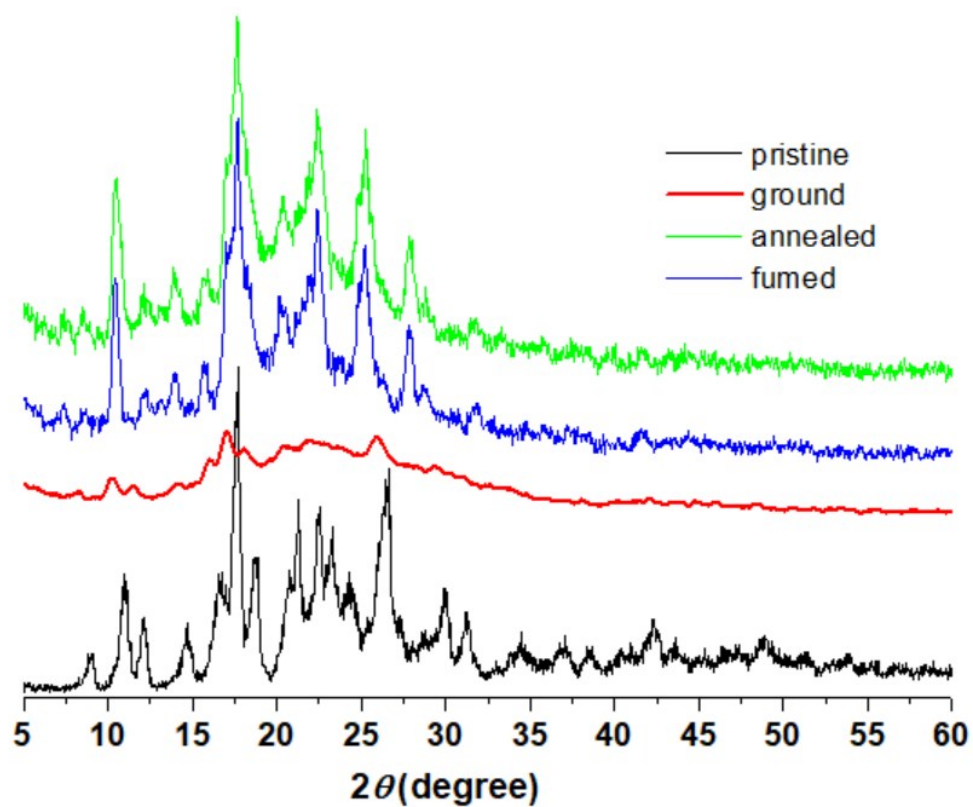
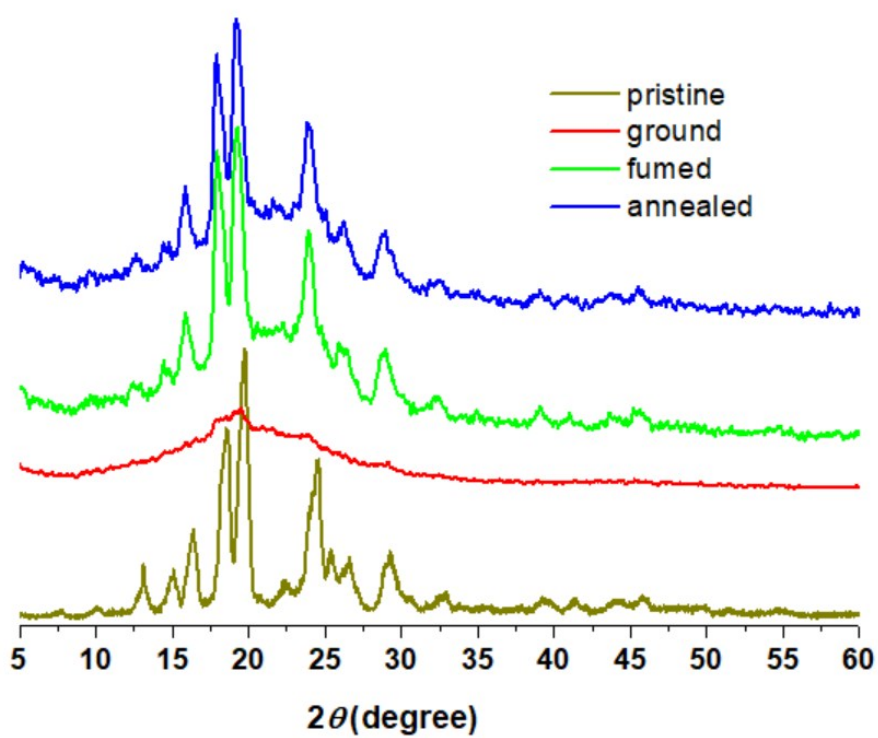


Fig. 18 Emission spectra ( $\lambda_{\text{ex}} = 365$  nm) of compound  $\text{V}_{\text{Ap}}$  under different solid-state conditions



**Fig. S19** PXRD patterns of compound  $V_O$  under different solid-state conditions





**Fig. S20** PXRD patterns of compound  $V_{Bp}$  under different solid-state conditions

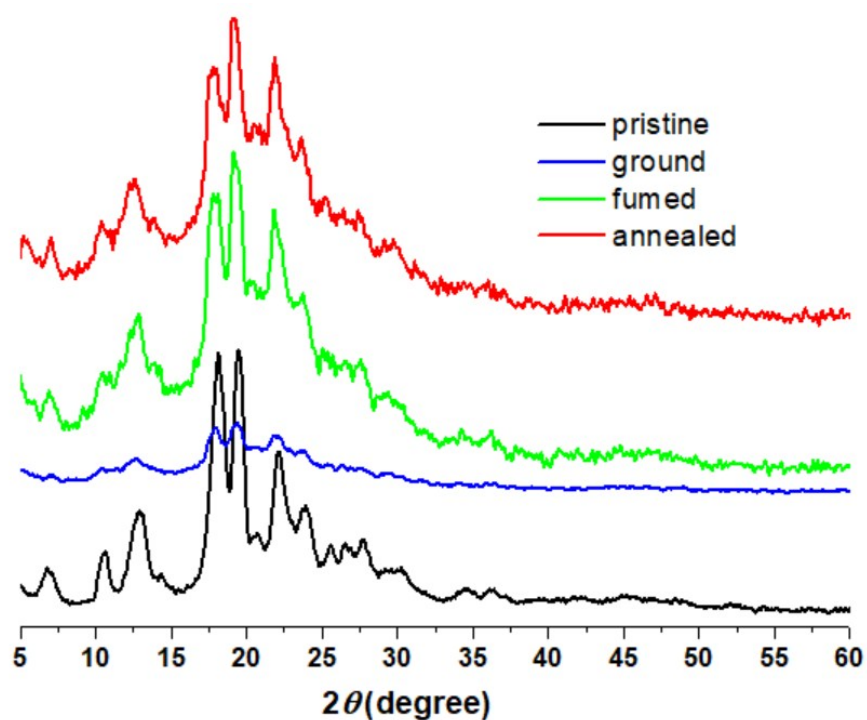


**Fig. S21** PXRD patterns of compound  $V_{Am}$  under different solid-state condition

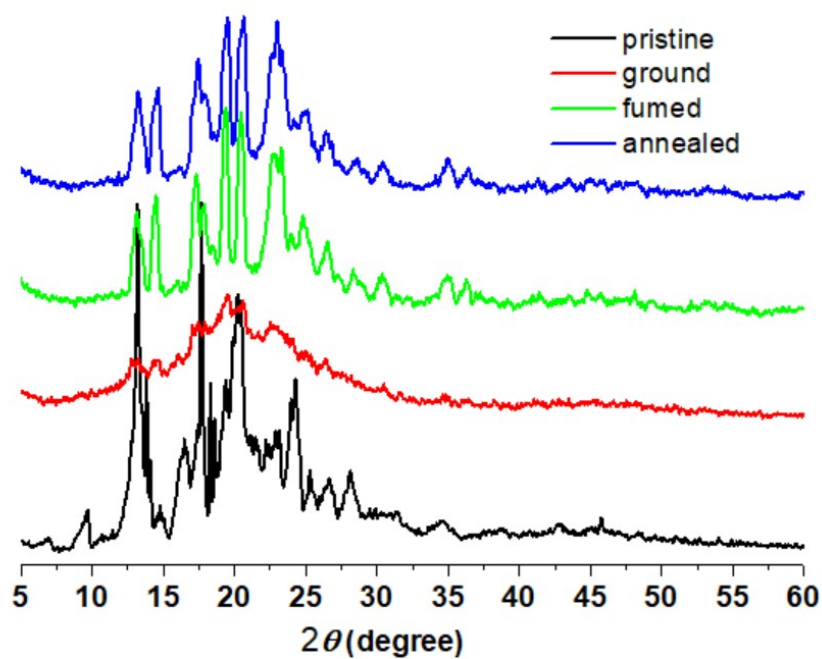


**Fig. S22** PXRD patterns of compound  $V_{Ap}$  under different solid-state condition

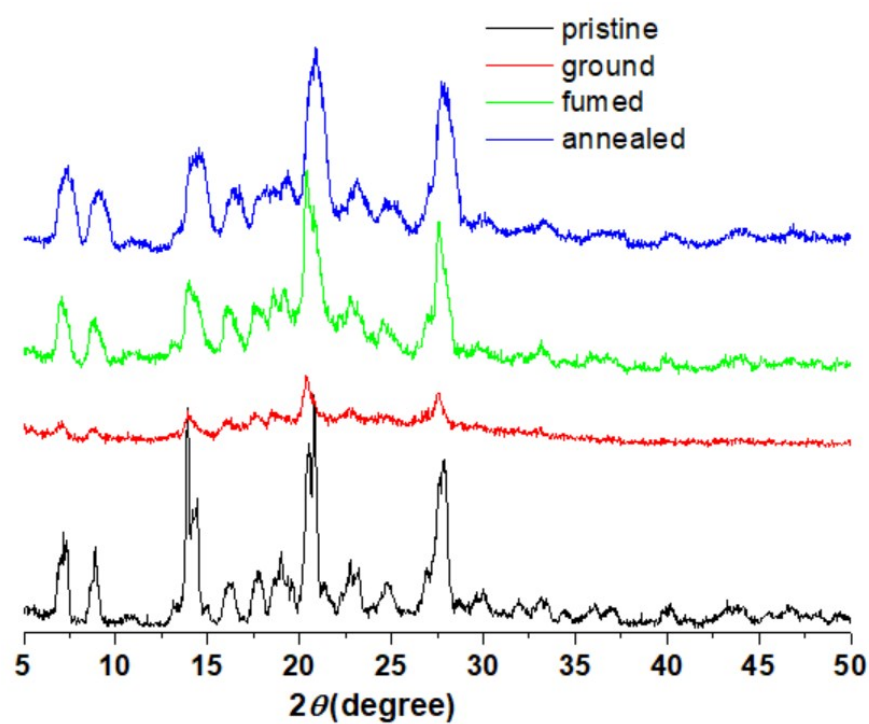


**Fig. S23** PXRD patterns of compound **V** under different solid-state conditions

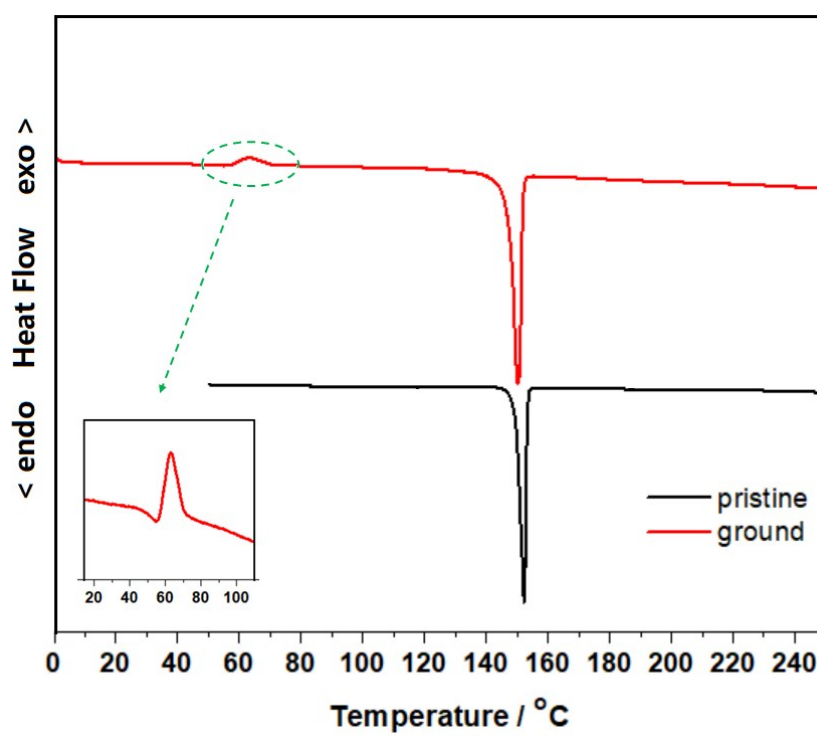


**Fig. S24** Differential scanning calorimetry curves of  $V_O$  under different solid-state conditions

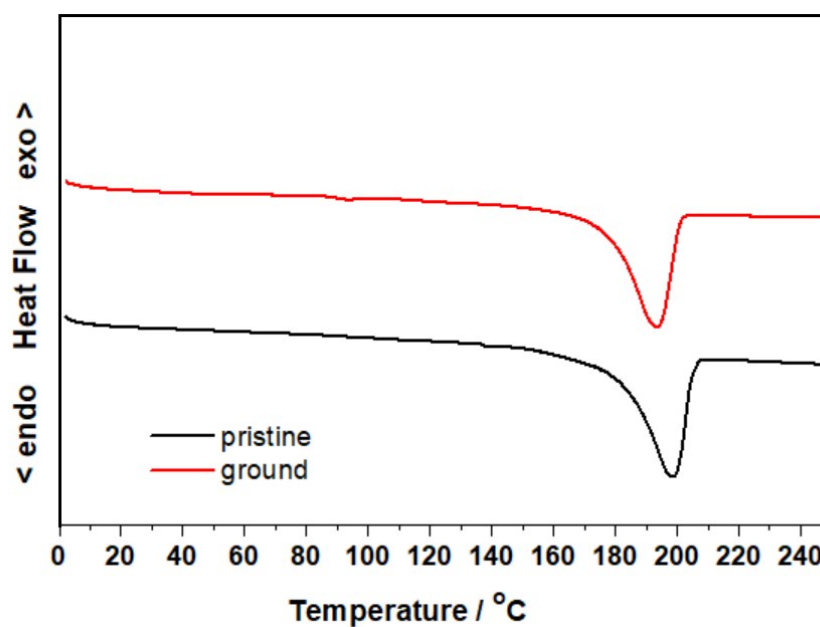


**Fig. S25** Differential scanning calorimetry curves of  $V_{Ap}$  under different solid-state conditions

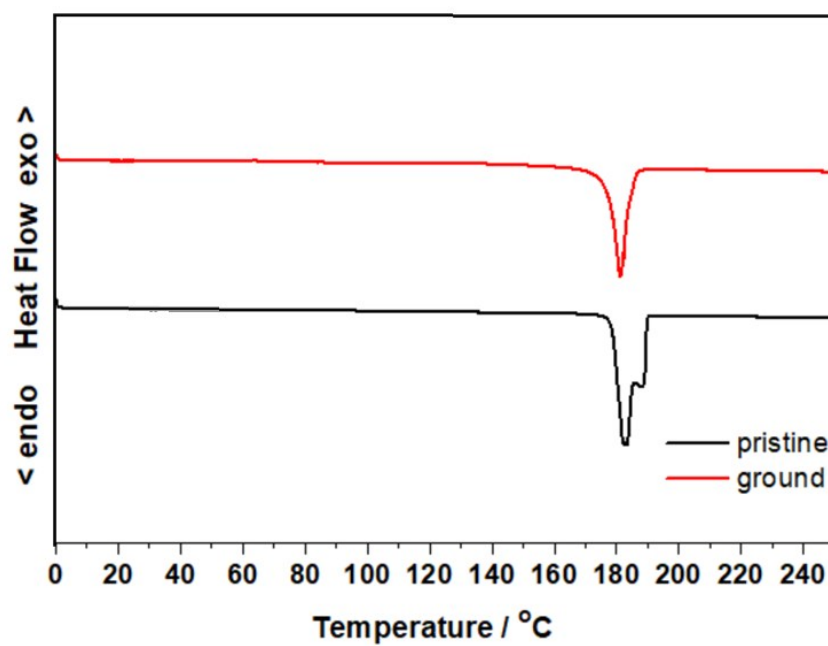


**Fig. S26** Differential scanning calorimetry curves of  $V_{Bp}$  under different solid-state conditions

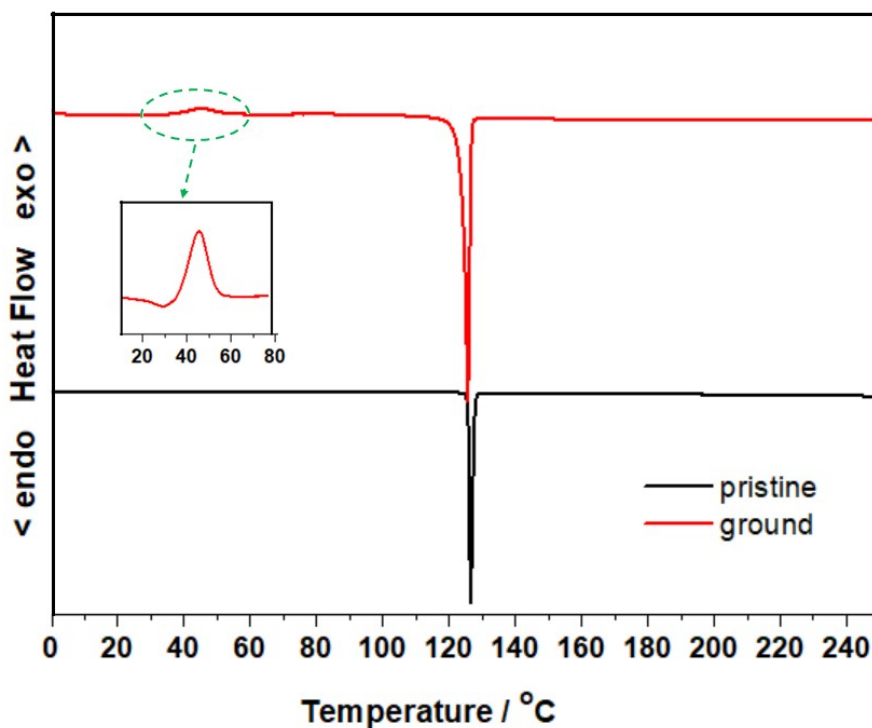


**Fig. S27** Differential scanning calorimetry curves of  $V$  under different solid-state conditions

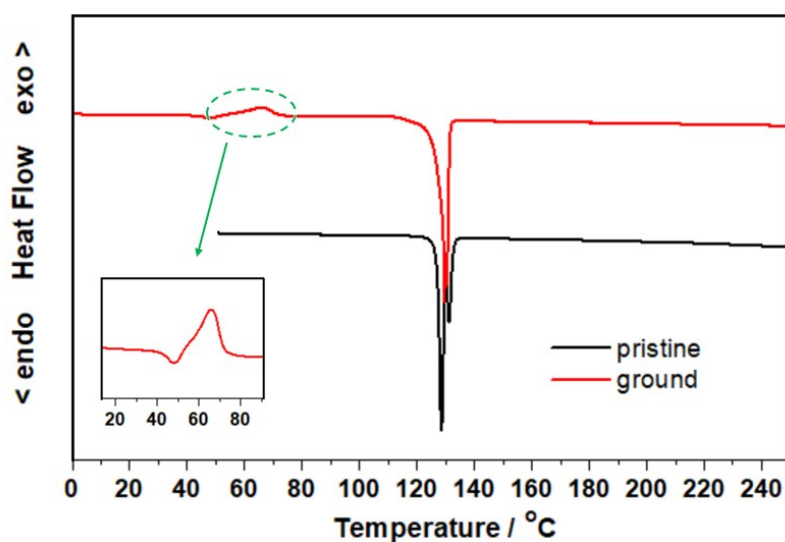


**Fig. S28** Differential scanning calorimetry curves of  $V_{Am}$  under different solid-state conditions

